Foot Shape Modeling

Ameersing Luximon and **Ravindra S. Goonetilleke,** Hong Kong University of Science and Technology, Clear Water Bay, Kowloon, Hong Kong

This study is an attempt to show how a "standard" foot can be parameterized using foot length, foot width, foot height, and a measure of foot curvature so that foot shape can be predicted using these simple anthropometric measures. The prediction model was generated using 40 Hong Kong Chinese men, and the model was validated using a different group of 25 Hong Kong Chinese men. The results show that each individual foot shape may be predicted to a mean accuracy of 2.1 mm for the left foot and 2.4 mm for the right foot. Application of this research includes the potential design and development of custom footwear without the necessity of expensive 3-D scanning of feet.

INTRODUCTION

The foot is a flexible structure, as 26 bones give its shape. Large deformations from its neutral posture, however, can place excessive stress and sometimes strain, giving rise to discomfort and even pain. Thus it becomes important to capture the 3-D shape of the foot in order to be able to design a suitable protective covering. The aim of this paper is to develop a method to predict the 3-D foot shape using anthropometric dimensions such that a last can be scientifically designed by having a one-to-one mapping from 3-D foot shape to 3-D last shape.

Because of rapid advancements in computer processing capabilities, there is a drive to replace the expert last maker with a computer designer (Lord, Foulston, & Smith, 1991). Studies such as that by Tsutsumi and Kouchi (1992) represented the 3-D shape of the foot using Bezier curves. Unfortunately, they did not discuss the accuracy of their foot model or the usefulness of the model for grading and sizing. Similarly, Yavatkar (1993) has modeled one individual's foot using I-DEAS graphics programming language. He generated a 3-D model of a foot by lofting four segments (forefoot to instep, instep to medial-lateral malleolus level, malleolus to lateral point of heel, and heel part) on the foot. The accuracy of the model was determined by comparing the volume "outside" the foot form and "inside" the foot form. The volume outside was around 50 000 mm^3, whereas the amount within the foot was approximately 27 000 mm^3. The generalizability of Yavatkar's model is relatively unknown, as only one foot was used for the predicted model. In a manufacturing context, Lord et al. (1991) discussed a computer-aided design system for the custom design of orthopedic shoe uppers, and Houle, Beaulieu, and Liu (1998) described a method to make custom footwear.

The paper uses B-spline surface modeling techniques, regression and recursive methods to generate a 3-D foot model using basic anthropometric measures. The extensively studied B-splines are used as a standard for surface representation in computer-aided engineering software (Choi, 1991; DeBoor, 1978), and B-splines are considered the most efficient curve or surface representation because of their useful properties, such as spatial uniqueness, boundedness and continuity, and local shape controllability (Bartels, Beatty, & Barsky, 1987). Recursive algorithms provide the flexibility to solve complex problems using very simple and efficient algorithms (Roberts, 1986), and regression methods are widely used to generate a polynomial equation between two or more variables (Johnson & Wichern, 1992). After the foot shape is

Address correspondence to Ravindra S. Goonetilleke, Dept. IEEM, HKUST, Clear Water Bay, Kowloon, Hong Kong; ravindra@ust.hk. **HUMAN FACTORS,** Vol. 46, No. 2, Summer 2004, pp. 304–315.

generated, the error between the predicted shape and the actual foot surface is represented using color coding, as shown in Luximon, Goonetilleke, and Tsui (2001). The advantage of the proposed method is that the same measures may also be used for sizing feet.

METHODOLOGY

Participants

All the participants in this experiment (65 Hong Kong Chinese men) were staff and students at the Hong Kong University of Science and Technology. Of these, 40 were used to generate the prediction model and 25 were used to validate the model. None of the participants had any foot illness or foot abnormalities, and each was paid HK$75 (~$10 U.S.) for his participation.

Procedure

Participant preparation and measurement. Each participant signed a consent form, after which his age, weight, and height were recorded. Their feet were washed and disinfected using an antiseptic germicide in a foot bubble roller massager. The water temperature was maintained at 25±1°C using a DigiSense® thermistor. After participants dried their feet, their foot length, arch length, and foot width were measured using the Brannock device while they stood on both feet.

Foot landmarking. There were 11 points marked on the foot (Figure 1): 7 on the metatarsal-phalangeal joint (MPJ), 2 on the dorsal surface of foot (Points 8 and 9), and 2 on the plantar side of the foot (Points 10 and 11). The last 4 points were chosen so that each scanned foot could be aligned during processing (see sections titled Metatarsal-Phalangeal Joint Equations and "Standard" Foot and Foot Shape Prediction Model). The MPJ points were used so that the MPJ line could be modeled using polynomial regression (see section titled Metatarsal-Phalangeal Joint Equations).

The MPJ landmarks (Figure 1) were identified by palpating the bony projections at the MPJ joints: five points on top (Points 2–6) and two points on the side of the first and fifth MPJ (Points 1 and 7). The two points on the dorsal side were marked using the foot-marking device (Ho, 1998). The participant placed one foot on the foot-marking device and the other foot on a platform at the same height. The participant's foot was aligned at the heel using a foot template positioned on the marking device. The foot length and width were measured on the foot-marking device. Points 8 and 9 were then located

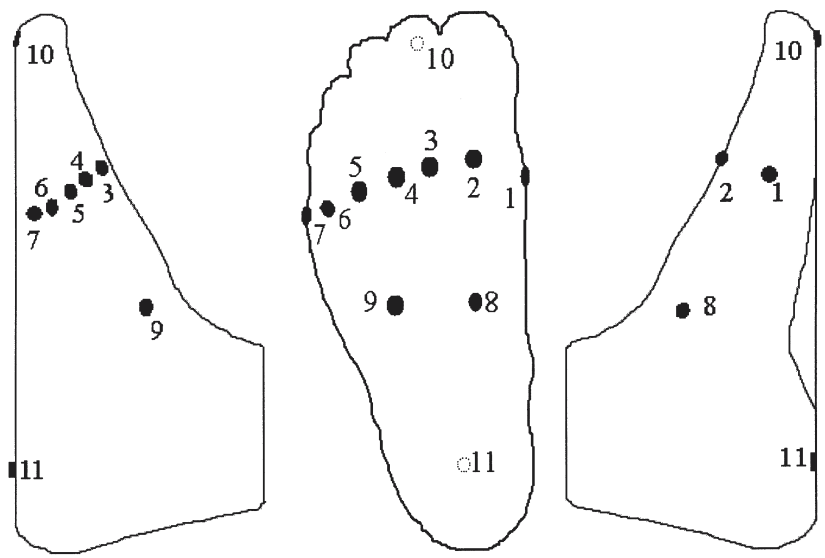

Figure 1. Landmark locations.

at 50% foot length along the length of the foot with angles of 30° (medial side) and –30° (lateral side), respectively.

The plantar surface points (Points 10 and 11) were located using a caliper and were marked with the foot off the marking device. Point 11 was at the center of the heel at 20% of foot length, and Point 10 was at the center of the second toe at 10 mm from the toe tip so that alignment with respect to the center of the second toe could be performed. After all the points were marked with a pen, 10-mm black stickers were placed at the center of the 11 "ink points."

Foot scanning and processing. The laser scanner calibration is dependent on color, and hence the participants wore a very thin white sock (0.2 mm). The sock was cut at the landmark locations so that the landmarks were directly visible. The scanner software can locate the center of the 10-mm black stickers, and thus the location of the landmarks could be identified. Each participant's feet were scanned using a Yeti 3-D laser scanner (Vorum Research Corporation, 1998). The participant stood with one foot on the glass platform inside the scanner and the other foot on a weighing scale (Figure 2) so that the weight was distributed equally on both feet. The scanned foot was first aligned using a "positioning ruler" and a foot template transparency.

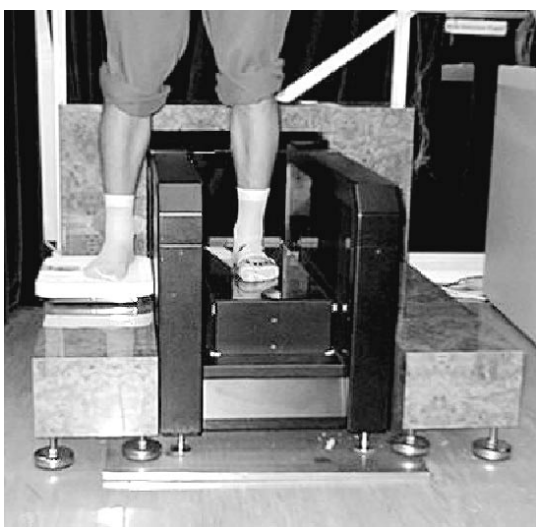

Figure 2. Participant standing with one foot in scanner and the other on a weighing scale.

The alignment tools were used to increase repeatability because the scanned data may show variations depending on the foot location even within the scanner. The foot was scanned and the procedure was repeated with the other foot.

The coordinates of the foot surface points and the 11 landmarks had the same coordinate system but were placed on separate layers of the data file. The total number of scanned points depended on the length of each foot, as the scan "sections" were set to be 1 mm apart. Thus the participants had differing numbers of sections and hence differing numbers of points, depending on their foot length.

The 3-D point cloud data were analyzed using MATLAB Version 5 with the Spline Toolbox. The shape of the MPJ curves was first determined, followed by a 3-D foot shape prediction using a parametric transformation of a "standard" foot shape. The model was validated using a different group of participants. The prediction model error was calculated using the dimensional difference between the predicted shape and the actual foot shape.

MODELING

Metatarsal-Phalangeal Joint Equations

The MPJ curve of the foot in two dimensions is very important, as the flex line of a shoe should match this curve. Hence only dimensions x and z (Figure 3) were used for the computation of the MPJ curve. In order to find this curve, we aligned the foot and landmarks (Figure 3) along the heel center (Point 11) to the second toe (Point 10) line (Tsutsumi & Kouchi, 1992). Points 10 and 11 were used to reduce the complexity and also to allow us to use the resulting equation without any additional manipulations. In other words, a local coordinate system was preferred to a global coordinate system for comparing among individuals. Using a coordinate axis transformation, the x and z coordinates of the landmarks were determined and normalized with respect to the length and width of each foot. In other words, the landmark coordinates were transformed as $x_{new} = (x - x_{min})/(x_{max} - x_{min})$ and $z_{new} = (z - z_{min})/(z_{max} - z_{min})$. Polynomial regression was then used on these normalized coordinates to determine the MPJ curve.

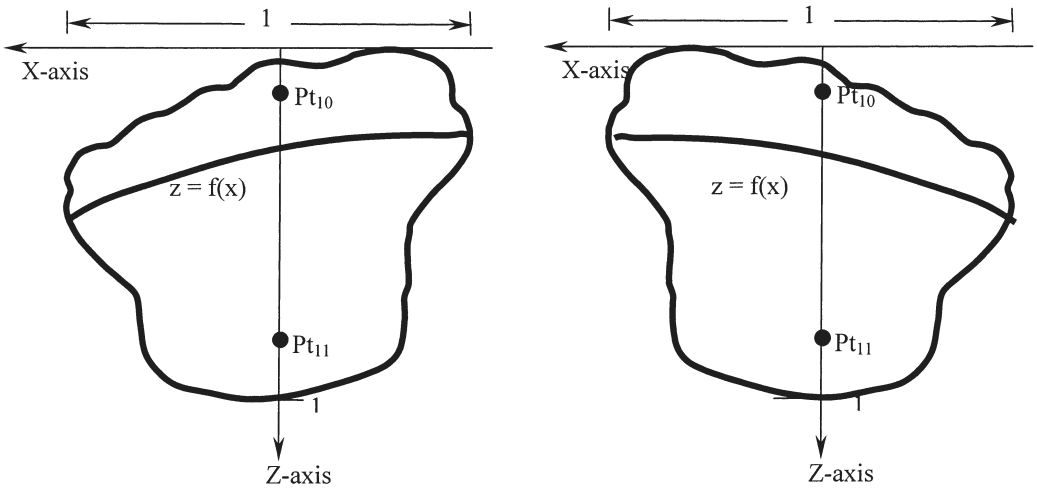

Figure 3. The MPJ curve of the foot after normalization with foot length along *z* axis and foot width along *x* axis.

"Standard" Foot and Foot Shape Prediction Model

The "standard" foot was generated using the 3-D foot shape data of the 40 participants. This procedure is shown in Figure 4 and described in detail in this section.

Alignment. In order to improve robustness, we used an alignment process slightly different from that of the two-point alignment used to determine the MPJ equation. As a first approximation, the line joining Points 8 and 9 was made parallel to a temporary *x* axis. Then the 2-D foot shape (or foot outline) was determined by extracting the points located on the circumference. Using this foot outline, we calculated the heel centerline (corresponding to 20% of foot length) and made this the *z* axis ("heel alignment" in Figure 4). The series of translations and rotations needed to transform the heel centerline to the *z* axis was stored, and then the complete 3-D foot shape was transformed with the same translations and rotations.

Section extraction. After alignment, each foot was divided into 99 sections (the interval between sections was equal to 1% of foot length) perpendicular to the heel centerline (i.e., *z* axis; Figure 5).

Section parameter determination. Each such section i had points $p_{ij} = (x_{ij}, y_{ij}, z_{ij})$, in which $i = 1,...,99$, $j = 1,...,360$. The lateral width (a_i), medial width (e_i) and height (h_i) were computed for each section (Figure 5). For the left foot, lateral width $(a_i) = max\{x_{ij}$ for $j = 1,...,360\}$ and medial width $(e_i) = |min\{x_{ij}$ for $j = 1,...,360\}|$. Similarly, for the right foot (note that the *max* for left foot is now *min* and *min* for left foot is *max*), lateral width $(a_i) = |min\{x_{ij}$ for $j = 1,...,360\}|$ and medial width $(e_i) = max\{x_{ij}$ for $j = 1,...,360\}$.

The width, w_i, of each section is the sum of the lateral and medial width ($w_i = a_i + e_i$). Foot flare ratio is "a measure of the deviation of the forepart of the foot with reference to the heel, and affords a useful index of the basic shape of the foot" (Freedman et al., 1946, p. 83). Thus the width ratio e_i/w_i provides information about the deviation of the forefoot from the heel centerline, or foot curvature or flare of the foot (Goonetilleke & Luximon, 1999). In other words, the width ratio changes as one moves from heel to toe, and this change can be used to quantify the foot curvature.

Recursive regression for the prediction of anthropometric measures. Because there are 99 sections, there are 99 w_i, 99 h_i, 99 a_i, and 99 e_i. To reduce the number of measures, we developed linear regression equations between the measures (a_i, e_i, w_i, and h_i) of section i and the measures (a_{i+1}, e_{i+1}, w_{i+1}, and h_{i+1}) of section i+1. Hence there were 98 linear regression equations

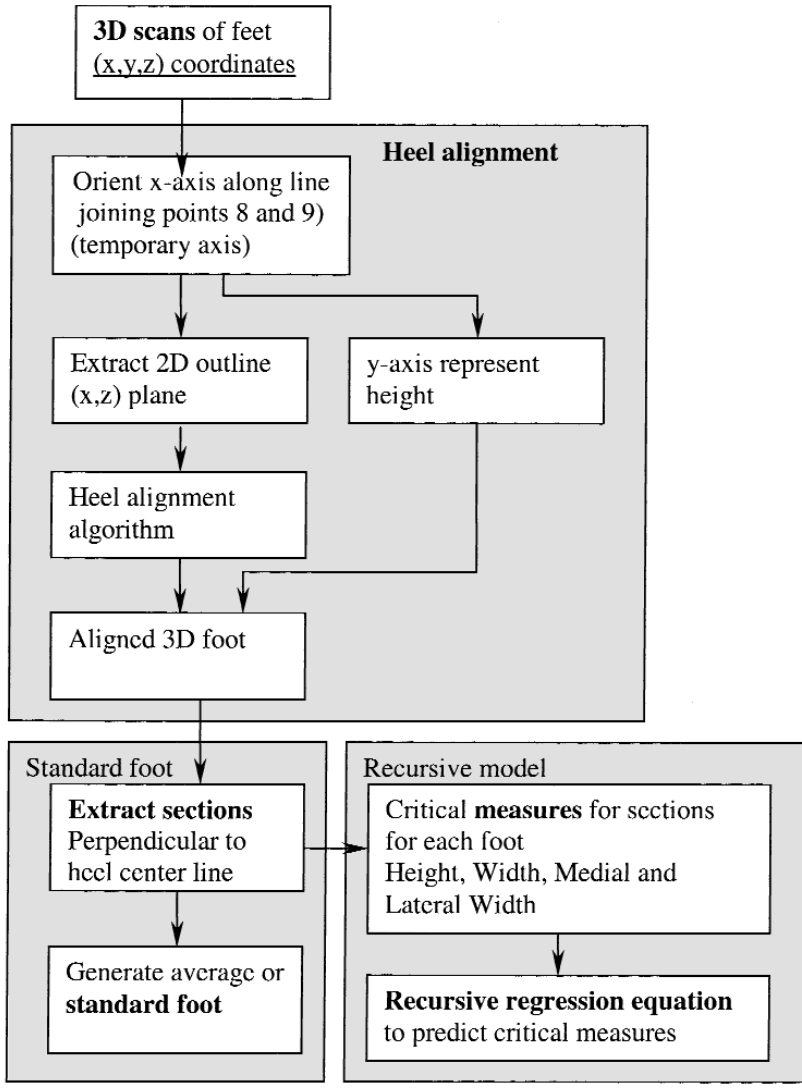

Figure 4. Flow chart to generate standard foot and recursive method.

between consecutive sections for the 99 h_i and a total of 98 × 4 linear regression equations for the four variables. Because only four parameters were used for the prediction, it is necessary to know the optimum starting or "seed" section for each dimension. If a section τ% on a foot was selected to be this seed, let the lateral width, medial width, width, and height of the seed section be a_τ, e_τ, w_τ, and h_τ, respectively.

The anthropometric values of the other sections (excluding section at τ% on foot) can then be predicted recursively using the aforementioned regression equations. Let the predicted anthropometric values be $\hat{e}_{i\tau}$, $\hat{a}_{i\tau}$, $\hat{w}_{i\tau}$, and $\hat{h}_{i\tau}$ when τ% of foot length is selected to be the seed section. Let the correlation coefficient between the predicted widths ($\hat{w}_{i\tau}$) and the actual widths (w_i) be ${}_wR_\tau^2$. When each of the sections $i = 1,...,99$ was used as the seed section, let the correlation coefficient between the predicted width and actual width be ${}_wR_i^2$. The mean correlation coefficient of the 40 participants was then determined as the mean ${}_wR_i^2$ of each foot (${}_w\bar{R}_i^2$). Similar computations were performed

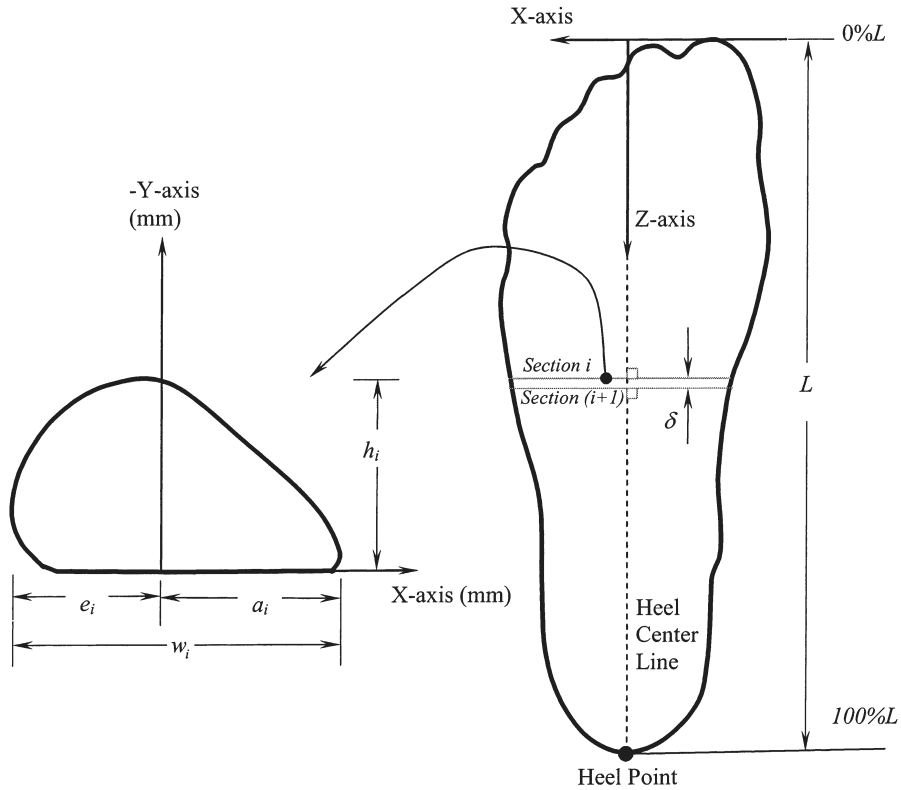

Figure 5. Model parameters for left foot.

to determine the mean correlation coefficient for lateral width, medial width, and height. Let these mean correlation coefficients be ${}_{a}\bar{R}_{i}^{2}$, ${}_{e}\bar{R}_{i}^{2}$, and ${}_{h}\bar{R}_{i}^{2}$. The optimum ("seed") section ($i = \mu$) that gave the maximum average correlation coefficient was chosen as the seed. The predicted lateral width, medial width, width, and height were then given by $\hat{a}_{i\mu}$, $\hat{e}_{i\mu}$, $\hat{w}_{i\mu}$, and $\hat{h}_{i\mu}$ when the optimum seed (μ) was used. The optimum seed section for the different anthropometric measures can be different.

Generating "standard" foot shape. The standard foot shape was generated using the mean cross sections of the 40 participants. For each section i, the center was given by $({}_{c}x_i, {}_{c}y_i, {}_{c}z_i)$, in which

$${}_{c}x_i = \sum_{j=1}^{360} \frac{x_{ij}}{360},$$

$${}_{c}y_i = \sum_{j=1}^{360} \frac{y_{ij}}{360},$$

and ${}_{c}z_i = i\%$ of foot length from minimum point along the z axis.

The center $({}_{c}x_i, {}_{c}y_i, {}_{c}z_i)$ of each section was aligned to the mean center of all the sections. Then, for each section, a smooth outline was generated using spline interpolation. For each section, the "radius," $r_{i\theta}$, was calculated at $\theta°$ intervals (where $\theta = 1°,...,360°$). The mean radius $\bar{r}_{i\theta}$ of all participants ($N = 40$) was then calculated. Based on a cylindrical-to-Cartesian coordinate transformation, the radius $\bar{r}_{i\theta}$ at $\theta°$, together with the z values, were converted into $(\bar{x}_{i\theta}, \bar{y}_{i\theta}, \bar{z}_{i\theta})$ coordinates. The standard foot shape then had 99 mean sections with points $\bar{p}_{i\theta}$ ($i = 1,...,99$; $\theta = 1°,...,360°$). The lateral width, medial width, width, and height of the standard foot were $\bar{a}_i, \bar{e}_i, \bar{w}_i$, and $\bar{h}_i$, respectively.

Modifying Standard Foot Shape Using Anthropometric Measures

The standard foot shape was scaled using the predicted anthropometric dimensions (Figure 6). If the predicted height of a section was $\hat{h}_{i\mu}$ and

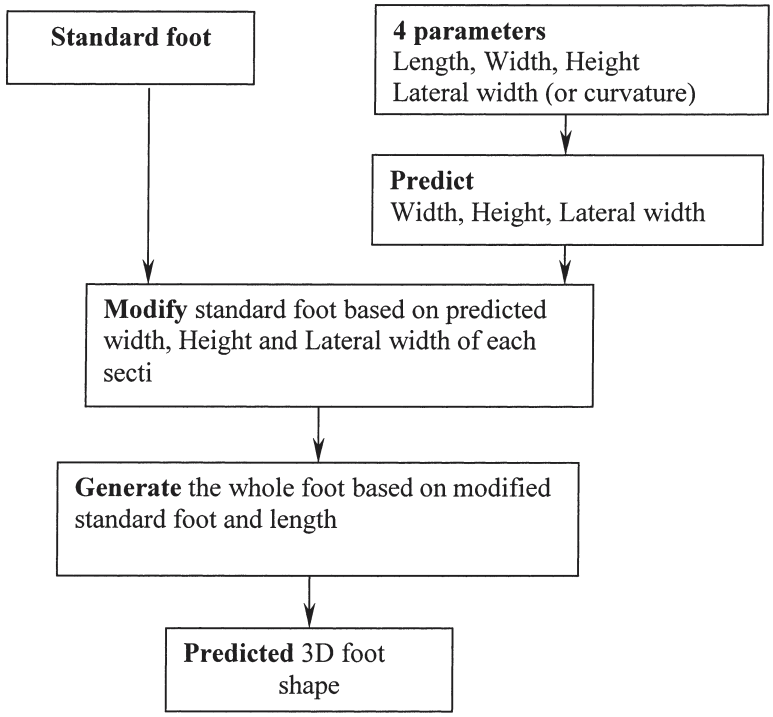

Figure 6. Flow chart showing how the standard foot was used to generate foot shape of an individual.

the height of the standard foot was $\bar{h}_i$, then the height scaling for the section was $(\hat{h}_{i\mu}/\bar{h}_i)$. Similarly, the width scaling was $(\hat{w}_{i\mu}/\bar{w}_i)$. All the y values $(\bar{y}_{i\theta})$ of the standard foot were scaled using height scaling and the x values $(\bar{x}_{i\theta})$ of the standard foot were scaled using width scaling (Figure 7). After height and width scaling, the points $(\bar{x}_{i\theta}, \bar{y}_{i\theta})$ were transformed to $[\bar{x}_{i\theta}(\hat{w}_{i\mu}/\bar{w}_i), \bar{y}_{i\theta}(\hat{h}_{i\mu}/\bar{h}_i)]$. The section was shifted based on the predicted lateral width $(\hat{a}_{i\mu})$. The predicted points were $\hat{p}_{i\vartheta} = (\hat{x}_{i\vartheta}, \hat{y}_{i\vartheta}, \hat{z}_{i\vartheta})$. If the four "seed" anthropometric measures are provided for one foot, then anthropometric measures of other sections can be predicted using the recursive regression equations. The length measure was included in the prediction model because the foot was sectioned at regular intervals along its length. Using the predicted anthropometric measures of each section and the length of the foot, the "standard" can be then be modified to give the (predicted) foot shape.

Accuracy of Model

The model was validated using the foot scans of 25 other participants. The error was computed based on the shortest distance from the predicted foot $(\hat{x}_{i\vartheta}, \hat{y}_{i\vartheta}, \hat{z}_{i\vartheta})$, in which $i = 1,...,99$ and $\vartheta = 1,...,360°$ to the actual foot $(\tilde{x}_{lm}, \tilde{y}_{lm}, \tilde{z}_{lm})$, in which $l = 1,...,S$ and $m = 1,...,360$. So, for a given point $(\hat{x}_{i\vartheta}, \hat{y}_{i\vartheta}, \hat{z}_{i\vartheta})$ on the predicted shape, the shortest distance $(e_{i\vartheta})$ to the actual foot shape was given by

$$e_{i\vartheta} = min\left\{\sqrt{(\tilde{x}_{lm}-\hat{x}_{i\vartheta})^2+(\tilde{y}_{lm}-\hat{y}_{i\vartheta})^2+(\tilde{z}_{lm}-\hat{z}_{i\vartheta})^2}\right\},$$

in which $l = 1,...,S$ and $m = 1,...,360$.

The mean error between predicted shape and actual shape of foot was then given by

$$\bar{e} = \frac{1}{99 \times 360}\sum_{i}^{90}\sum_{\vartheta}^{360} e_{i\vartheta}.$$

The maximum and minimum of the error were also recorded, together with the mean error.

RESULTS

The letter symbols of the Brannock width unit were converted to numeric units (Table 1).

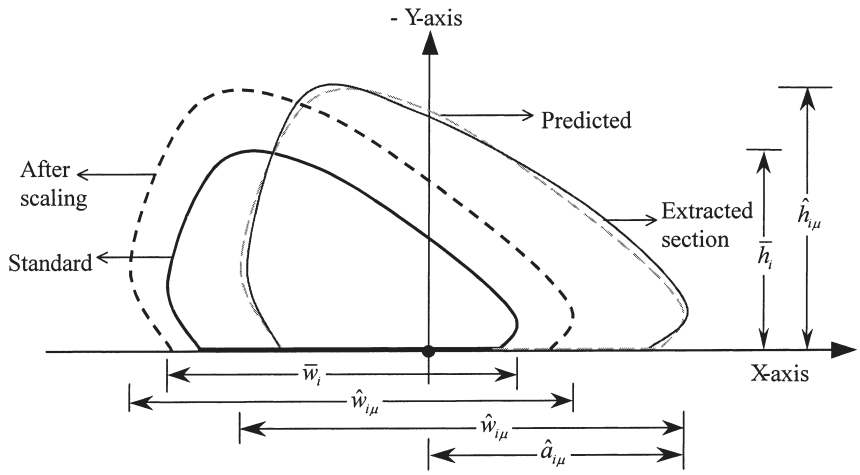

Figure 7. Generation of predicted section from standard section.

The simple statistics of the participants on whom the prediction model was based are shown in Table 2, and the simple statistics of the participants who were used to validate the prediction model appear in Table 3. Figure 3 shows the location of the MPJ curve, and the modeled polynomial equations are given in Table 4. The MPJ curve was modeled using polynomial of Orders 2, 3, and 4, and it was found that the polynomial of Order 4 could explain more than 82% of the variation in both feet (Table 4).

Figure 8a shows the plot of the mean correlation coefficient ${}_{w}\bar{R}_{i}^{2}$ between the predicted width and actual width of the right and left foot against the seed section *i*. In Figure 8a, the maximum ${}_{w}\bar{R}_{i}^{2}$ occurred at $i = 9\%$ for both the left and right feet. Figures 8b, 8c, and 8d show the plots of the mean correlation coefficients ${}_{a}\bar{R}_{i}^{2}$, ${}_{e}\bar{R}_{i}^{2}$, and ${}_{h}\bar{R}_{i}^{2}$ related to the lateral width, medial width, and height. The maximum of ${}_{a}\bar{R}_{i}^{2}$ occurred

TABLE 1: Number Assignment to Brannock Width

Brannock Width	Assigned Value
AAA	1
AA	2
A	3
B	4
C	5
D	6
E	7
EE	8
EEE	9

TABLE 2: Simple Statistics of Participants Used to Develop the Model ($n = 40$)

	Mean	Max.	Min.	*SD*
Age (years)	22	36	19	3.4
Weight (kg)	63	90	47	8.5
Height (cm)	171.3	183.4	160.1	5.55

	Right Foot				Left Foot			
	Mean	Max.	Min.	*SD*	Mean	Max.	Min.	*SD*
Foot length (Brannock)	8.6	13.0	6.5	1.38	8.5	13.3	5.3	1.47
Foot length (cm)	24.6	27.3	22.5	1.11	24.0	27.3	1.5	3.81
Foot width (Brannock)	5.4	7.5	3.0	0.96	5.6	8.5	3.5	0.98
Foot width (cm)	9.9	11.2	9.0	0.50	10.0	11.6	9.0	0.51
Arch length (Brannock)	9.4	15.0	6.5	1.72	9.0	15.0	5.5	1.80

TABLE 3: Simple Statistics of Participants Used to Validate the Model (n = 25)

	Mean	Max.	Min.	*SD*
Age (years)	21.6	41.0	19.0	4.3
Weight (kg)	65.2	88.3	47.4	8.6
Height (cm)	173.8	184.2	161.3	5.75

	Right Foot				Left Foot			
	Mean	Max.	Min.	*SD*	Mean	Max.	Min.	*SD*
Foot length (Brannock)	8.9	11.5	6.5	1.23	8.8	11.0	6.0	1.24
Foot length (cm)	25.1	26.8	23.5	0.98	25.0	26.8	22.8	1.09
Foot width (Brannock)	5.2	6.5	3.5	0.83	5.6	7.5	4.0	0.83
Foot width (cm)	10.0	11.2	9.0	0.40	10.0	11.2	9.2	0.42
Arch length (Brannock)	9.9	12.5	7.0	1.39	9.4	12.0	6.5	1.47

at i = 8% for the left foot and 7% for the right foot, as shown in Figure 8b. Similarly, it can be seen from Figure 8c that the maximum of ${}_{e}\bar{R}_i^2$ occurred at i = 9% for the left foot and 10% for the right foot. From Figure 8d, it can be seen that the maximum of ${}_{h}\bar{R}_i^2$ occurred at i = 52% for the right foot and 55% for the left foot, and for i > 60% the average ${}_{h}\bar{R}_i^2$ deteriorated because the height at the lower leg was assigned a fixed height. So the optimum seed to predict the left foot is to use the height at μ = 55, width at μ = 9, and lateral width at μ = 8. The optimum seed to predict the right foot is to use the height at μ = 52, width at μ = 9, and lateral width at μ = 7.

Using the optimum seed sections, we predicted the anthropometric dimensions, which were in turn used to modify the standard foot in order to generate the 3-D foot shape. The error between the predicted shape of the foot and the actual foot was computed. The mean, maximum, and minimum errors for the 25 participants' left and right feet were calculated and are shown in Table 5. The average error was 2.1 mm (SD = 0.79 mm) for the left foot and 2.4 mm (SD = 0.85 mm) for the right foot. The error plot for one participant is shown in Figure 9. In the plot, the different magnitudes of the error have been "color" coded using gray levels.

DISCUSSION

The objective of this paper was to determine whether a parametric approach to foot shape prediction was possible. The results show that the foot shape may be predicted to a mean accuracy of 2.1 mm for the left foot and 2.4 mm for the right foot. The prediction model may be improved by using more participants. However, different standard feet may be necessary to account for differences in age, gender, race, and so on. Assuming that the shape of the "standard" foot is known for different ages, genders, and races, a few anthropometric dimensions can help predict the 3-D foot shape for a specific

TABLE 4: Polynomial Regression Equations to Determine the MPJ Curve

Left Foot:
$z = 0.267^{*}x^2 + 0.103^{*}x + 0.259^{*}$, $R^2 = .816$, $p < .001$
$z = -0.226^{*}x^3 + 0.293^{*}x^2 + 0.142^{*}x + 0.256^{*}$, $R^2 = .826$, $p < .001$
$z = -1.729^{*}x^4 - 0.022x^3 + 0.701^{*}x^2 + 0.115^{*}x + 0.245^{*}$, $R^2 = .874$, $p < .001$

Right Foot:
$z = 0.272^{*}\ x^2 - 0.100^{*}x + 0.256^{*}$, $R^2 = .7512$, $p < .001$
$z = 0.223^{*}x^3 + 0.303^{*}\ x^2 - 0.138^{*}x + 0.254^{*}$, $R^2 = .7647$, $p < .001$
$z = -1.746^{*}x^4 + 0.031x^3 + 0.709^{*}x^2 - 0.106^{*}x + 0.243^{*}$, $R^2 = .8202$, $p < .001$

*Values are coefficients that are statistically significant at $p < .001$.

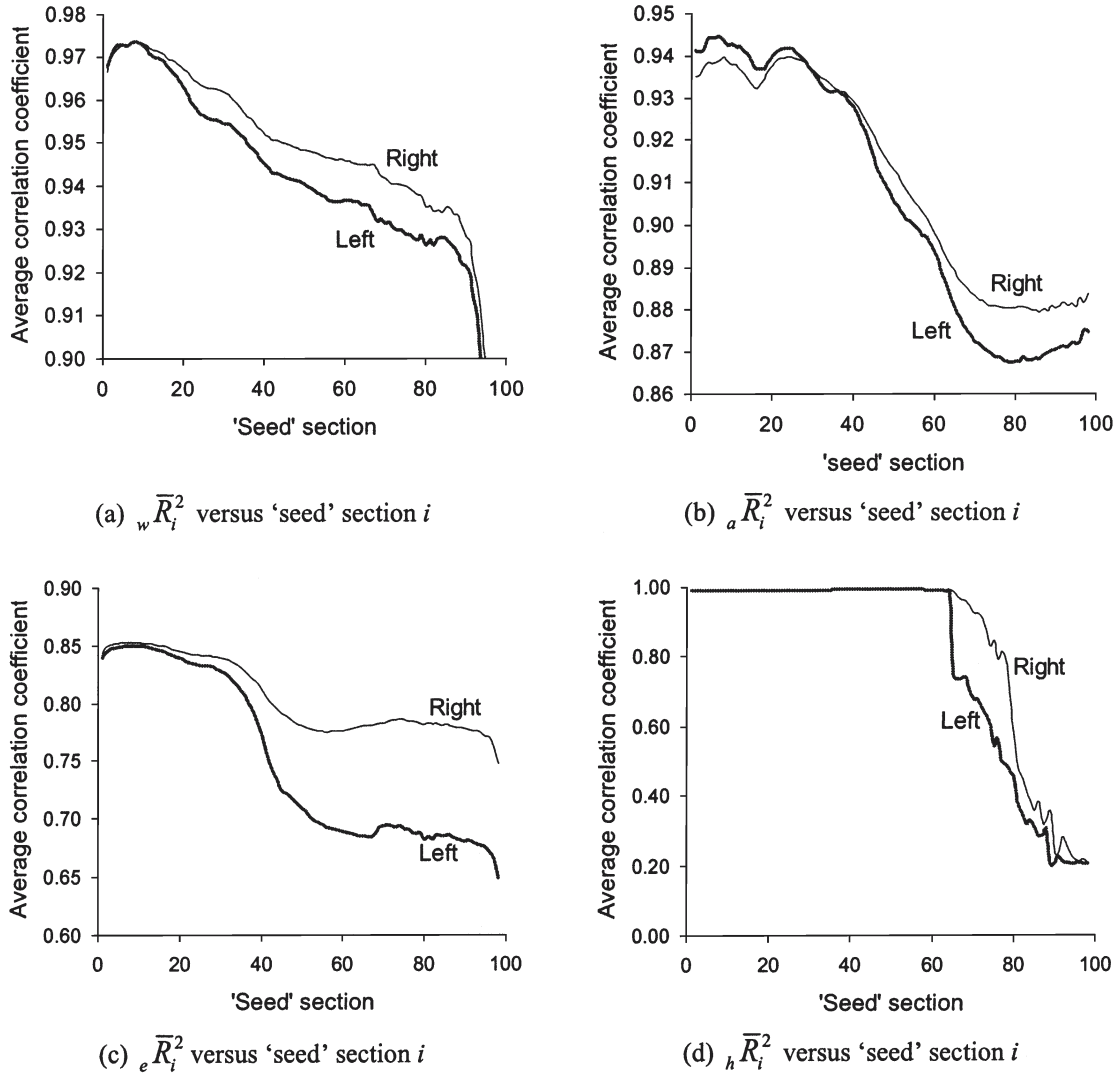

(a) ${}_{w}\overline{R}_i^2$ versus 'seed' section i

(b) ${}_{a}\overline{R}_i^2$ versus 'seed' section i

(c) ${}_{e}\overline{R}_i^2$ versus 'seed' section i

(d) ${}_{h}\overline{R}_i^2$ versus 'seed' section i

Figure 8. Mean correlation coefficient versus "seed" section i for left and right feet.

person. The predicted foot shape may be useful for the generation of a personalized last or in the selection of a suitable last to develop a customized shoe with only a limited number of dimensions.

The predictive model resulted in higher negative errors around the medial and lateral malleolus. These errors are most probably attributable to movement or change in a participant's posture while standing during scanning. This error may be reduced if the participant's posture during measurement can be controlled effectively.

The predicted width at the heel region had higher errors attributable to error propagation with the use of forward recursive regression because the seed section for the width calculation was based on the toe region. The error may be reduced if both forward (from toe) and backward (from heel) calculations are performed until the results converge within a specific tolerance. The backward calculation can consider a seed section around the heel and thus will counteract the effect of the forward prediction, thereby reducing the error and eventually improving the prediction accuracy. Around the heel, there was a positive error when predicting height. In the lower leg region around the ankle, the scanned height is a constant and is a function of the scanner itself, which resulted in poor prediction at the heel region. Using height

TABLE 5: Mean, Minimum, and Maximum Error (mm) Between the Predicted and Actual Feet of 25 Participants

	Left			Right		
Participant	Mean	Min.	Max.	Mean	Min.	Max.
1	2.3	–6.7	9.4	2.2	–7.8	8.2
2	1.5	–5.8	5.4	1.6	–4.9	6.6
3	2.8	–13.6	14.0	1.6	–8.1	5.8
4	1.4	–3.0	5.1	2.1	–4.8	8.6
5	3.2	–6.4	17.6	2.8	–8.7	17.7
6	1.4	–8.4	5.8	1.5	–7.3	6.5
7	1.5	–5.3	6.6	1.2	–4.0	5.9
8	1.8	–3.6	6.0	3.8	–9.1	13.4
9	3.7	–15.0	13.3	3.9	–12.9	15.3
10	1.6	–7.1	4.5	3.3	–8.9	24.5
11	3.2	–8.8	11.0	3.8	–12.9	13.2
12	1.6	–3.6	5.8	2.8	–8.6	10.8
13	2.6	–7.6	6.6	2.3	–8.3	6.9
14	3.1	–11.0	9.8	3.1	–9.5	9.3
15	2.4	–7.7	8.8	3.2	–9.2	14.8
16	3.9	–17.2	12.9	3.3	–10.9	9.4
17	1.6	–7.2	6.9	3.2	–12.4	12.2
18	1.9	–4.4	5.6	1.6	–4.6	11.3
19	1.8	–3.1	6.6	2.2	–5.1	9.3
20	1.3	–2.6	5.7	1.5	–3.7	6.3
21	2.2	–9.2	9.7	1.6	–8.9	7.5
22	1.4	–4.0	13.9	1.5	–3.5	11.8
23	2.7	–8.0	12.2	2.3	–5.5	10.7
24	1.4	–5.0	4.2	1.6	–5.5	5.8
25	1.5	–8.1	7.1	2.1	–12.1	9.9
Mean	2.1	–7.3	8.6	2.4	–7.9	10.5
Max.	3.9	–2.6	17.6	3.9	–3.5	24.5
Min.	1.3	–17.2	4.2	1.2	–12.9	5.8
SD	0.79	3.74	3.63	0.85	2.94	4.37

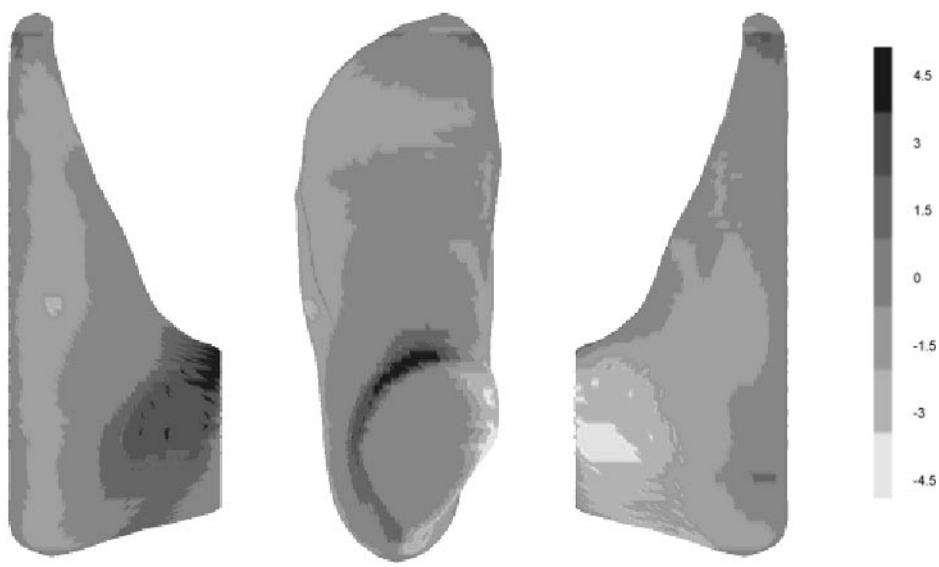

Figure 9. Predicted shape of foot with gray-scale-coded error. Scale values are in millimeters.

information along the foot length, a fictitious continuous curve could be generated for the lower leg region. This may improve the height prediction in the heel region.

In this model, foot sections were taken at a fixed percentage of the foot length. Because of differences in foot shape, sections at a given percentage of foot length may not be similar among feet. Therefore an improvement may have to be made to account for these differences or to find the best match of the sections for different feet. In the aforementioned method, the sections from the standard foot were scaled proportionately. Other types of scaling can be employed if different feet can be clustered and categorized.

In the prediction model and error computation, we used a fixed number of sections and points. If the optimum number of sections and points needed is determined, the accuracy of the model may be further enhanced. In addition, higher-order polynomial regression, instead of linear regression, may improve prediction accuracy further.

CONCLUSIONS

In this study, four anthropometric measures (length, width, height, and a measure of curvature) and a standard foot shape were used to predict the 3-D shape of a given foot. The four anthropometric measures were used to predict the anthropometric measures of 98 cross sections of a foot using recursive regression equations. A standard foot shape was generated after averaging the normalized foot shapes of 40 Hong Kong men. The method was validated using 25 Hong Kong men. Mean accuracies of 2.1 mm for the left foot and 2.4 mm for the right foot were obtained. Several methods to improve the prediction model have been discussed, including a differing standard foot shape for differing populations. This research may be used to develop custom lasts for the manufacture of custom footwear without actually scanning a person's feet.

ACKNOWLEDGMENTS

The authors would like to thank the Research Grants Council of Hong Kong for funding this study under Grant HKUST 6074/99E.

REFERENCES

Bartels, R. H., Beatty, J. C., & Barsky, B. A. (1987). *An introduction to splines for use in computer graphics and geometric modeling.* San Francisco: Morgan Kaufmann.

Choi, B. K. (1991). *Surface modeling for CAD/CAM: Advances in industrial engineering* (Vol. 11). Amsterdam: Elsevier.

DeBoor, C. (1978). A *practical guide to splines.* New York: Springer-Verlag.

Freedman, A., Huntington, E. C., Davis, G. C., Magee, R. B., Milstead, V. M., & Kirkpatrick, C. M. (1946). *Foot dimensions of soldiers* (Third Partial Report, Project No. T-13). Fort Knox, KY: Armored Medical Research Laboratory.

Goonetilleke, R. S., & Luximon, A. (1999). Foot flare and foot axis. *Human Factors, 41,* 596–606.

Ho, C.-F. (1998). *3-Dimensional foot digitization.* Unpublished master's thesis, Department of Industrial Engineering and Engineering Management, Hong Kong University of Science and Technology, Hong Kong.

Houle, P.-S., Beaulieu, E., & Liu, Z. (1998). Novel fully integrated computer system for custom footwear: From 3D digitization to manufacturing. In *Proceedings of the International Society for Optical Engineering: Three-dimensional image capture and applications* (pp. 65–73). San Jose, CA: SPIE – The International Society for Optical Engineering.

Johnson, R. A., & Wichern, D. W. (1992). *Applied multivariate statistical analysis.* Englewood Cliffs, NJ: Prentice-Hall.

Lord, M., Foulston, J., & Smith, P. J. (1991). Technical evaluation of a CAD system for orthopaedic shoe-upper design. *Journal of Engineering in Medicine, 205*(H2), 109–115.

Luximon, A., Goonetilleke, R. S., & Tsui, K. L. (2001). A fit metric for footwear customization. In *Proceedings of the 2001 World Congress on Mass Customization and Personalization* [CD-ROM]. Hong Kong: Hong Kong University of Science and Technology.

Roberts, E. (1986). *Thinking recursively.* New York: Wiley.

Tsutsumi, E., & Kouchi, M. (1992). Geometric modeling of the foot. In *Proceedings of the Fifth ASEE International Conference ECGDG 1992* (pp. 171–174). Washington, DC: American Society for Engineering Education, Engineering Design Graphics Division.

Vorum Research Corporation. (1998). *On-line help for Yeti shape builder Version 3.0* (Document Number 2700-8801-01). Vancouver, Canada: Author.

Yavatkar, A. S. (1993). *Computer aided system approach to determine the shoe-last size and shape based on statistical approximated model of a human foot.* Unpublished master's thesis, Tufts University, Medford, MA.

Ameersing Luximon received his Ph.D. in industrial engineering and engineering management from the Hong Kong University of Science and Technology in 2001. He is a postdoctoral research fellow at the Jockey Club Rehabilitation Engineering Center at Hong Kong Polytechnic University.

Ravindra S. Goonetilleke is an associate professor in the Department of Industrial Engineering and Engineering Management at the Hong Kong University of Science and Technology. He received his Ph.D. in human factors engineering from the State University of New York at Buffalo in 1990.

Date received: September 17, 2002
Date accepted: December 18, 2002